



**HAL**  
open science

## Tropical Wave Observations From the Reel-Down Atmospheric Temperature Sensor (RATS) in the Lowermost Stratosphere During Strateole-2

Martina Bramberger, Doug Goetz, M. Joan Alexander, Lars Kalnajs, Albert Hertzog, Aurelien Podglajen

► **To cite this version:**

Martina Bramberger, Doug Goetz, M. Joan Alexander, Lars Kalnajs, Albert Hertzog, et al.. Tropical Wave Observations From the Reel-Down Atmospheric Temperature Sensor (RATS) in the Lowermost Stratosphere During Strateole-2. *Geophysical Research Letters*, 2023, 50 (17), 10.1029/2023GL104711 . hal-04297087

**HAL Id: hal-04297087**

**<https://hal.science/hal-04297087v1>**

Submitted on 21 Nov 2023

**HAL** is a multi-disciplinary open access archive for the deposit and dissemination of scientific research documents, whether they are published or not. The documents may come from teaching and research institutions in France or abroad, or from public or private research centers.

L'archive ouverte pluridisciplinaire **HAL**, est destinée au dépôt et à la diffusion de documents scientifiques de niveau recherche, publiés ou non, émanant des établissements d'enseignement et de recherche français ou étrangers, des laboratoires publics ou privés.

1  
2  
3  
4  
5  
6  
7  
8  
9  
10  
11  
12

# Tropical wave observations from the Reel-down Atmospheric Temperature Sensor (RATS) in the lowermost stratosphere during Strateole-2

Martina Bramberger<sup>1</sup>, Doug Goetz<sup>2</sup>, M. Joan Alexander<sup>1</sup>, Lars Kalnajs<sup>2</sup>,  
Albert Hertzog<sup>3</sup>, Aurelien Podglajen<sup>3</sup>

<sup>1</sup>NorthWest Research Associates, Boulder Office, Colorado, USA

<sup>2</sup>Laboratory for Atmospheric and Space Physics, University of Colorado, Boulder, CO, USA

<sup>3</sup>Laboratoire de Météorologie Dynamique, Ecole Polytechnique, Palaiseau, France

## Key Points:

- high-resolution observations in the lowermost stratosphere from a new instrument
- Instrument detected tropical waves at resolution limit of reanalyses
- ERA5 reproduces waves, but temporal evolution differs from observations

---

Corresponding author: Martina Bramberger, [martina@nwra.com](mailto:martina@nwra.com)

**Abstract**

Tropical waves play an important role in driving the quasi-biennial oscillation (QBO) of zonal winds in the tropical lower stratosphere. In our study we analyze these waves based on temperature observations from the 2021-2022 Strateole-2 campaign when the Reel-down Atmospheric Temperature Sensor (RATS) was successfully deployed for the first time. RATS provides long-duration, continuous and simultaneous high-resolution temperature observations at two altitudes (balloon float level and 200m below) allowing for an analysis of vertical wavelengths. This separation distance was chosen to focus on waves near the resolution limit of reanalyses. Here, we found tropical waves with periods between about 6 hours and 2 days, with vertical wavelengths between 1.5 km and 5 km, respectively. Comparing our results to ERA5 reanalyses we found good agreement for waves with a period longer than one day. However, the ERA5 amplitudes of high-frequency waves are under-estimated, and the temporal evolution of most wave packets differs from the observations.

**Plain Language Summary**

We present measurements from the maiden flight of the RATS instrument (Reel-down Atmospheric Temperature Sensor) in November/December 2021. The instrument lowered a temperature sensor down to about 200 m from a balloon floating at about 18 km. By combining the temperature measurements at balloon floating level and RATS we analyze tropical waves with relatively small vertical wavelengths (<6 km). These waves are important as they drive the quasi-biennial oscillation in the east-west winds in the tropical stratosphere. This oscillation is acknowledged as an important process for seasonal forecasts, but it is currently not well resolved in weather or seasonal forecast models. In our study we compare the observed waves with waves in one weather model system (ERA5) and find that the spectral energies are similar for long-period waves (>1 day). However, the high-frequency waves (that provide about 25% of the necessary QBO forcing) are under-estimated by ERA5, which is likely related to the limited vertical resolution.

**1 Introduction**

Strateole-2 is a French-US project with a focus on dynamics, microphysics and composition in the tropical upper troposphere and lower stratosphere using long-duration superpressure balloons. Measurements include winds, temperatures, composition, clouds and aerosols from a variety of in situ and remote sensing instruments (Haase et al., 2018; Corcos et al., 2021; Kalnajs et al., 2021; Goetz et al., 2023). One goal is improved characterization of tropical waves, which drive variability in temperature and high cirrus clouds that have impacts on global stratospheric water vapor and decadal-scale climate variability (J.-E. Kim et al., 2016; Jensen et al., 2017; Solomon et al., 2010)

Tropical waves also drive the Quasi-Biennial Oscillation (QBO) in lower stratospheric zonal winds, a circulation with notable impacts on long-range prediction (Scaife et al., 2022). Global model systems struggle to simulate these climate processes (Richter, Anstey, et al., 2020; Davis et al., 2017), likely in part due to poor resolution of the short horizontal and/or vertical scales of important tropical waves (Holt et al., 2020; Richter, Butchart, et al., 2020; J.-E. Kim & Alexander, 2015; Bramberger et al., 2022).

To study the effects of tropical waves on QBO and cirrus clouds, global reanalyses provided by different centers for numerical weather prediction have been widely used (Ern et al., 2014; Y.-H. Kim & Chun, 2015; Pahlavan, Fu, et al., 2021; Pahlavan, Wallace, et al., 2021; Ueyama et al., 2023). Due to its higher horizontal resolution compared to its predecessors, the fifth generation European Centre for Medium-Range Weather Forecasts (ECMWF) Reanalysis (ERA5) is capable to resolve a wider spectrum of tropical

61 waves. This also allows for an improved representation of the wave-mean flow interac-  
 62 tion which is crucial for the generation of the QBO (Pahlavan, Fu, et al., 2021).

63 Recently, balloon studies have shown the importance of very short vertical wave-  
 64 length 1-5 day intrinsic period gravity waves with momentum fluxes that will contribute  
 65 substantial forces to the QBO in the lower stratosphere (Vincent & Alexander, 2020; Bram-  
 66 berger et al., 2022). These studies highlighted limitations of vertical resolution in reanal-  
 67 yses for representing short-vertical scale tropical waves, even for the high ( $\sim 350\text{m}$ ) res-  
 68 olution of ERA5. Together with modeling studies these observations highlight the im-  
 69 portance of high vertical resolution in the realistic representation of the QBO (Garfinkel  
 70 et al., 2022).

71 Motivated by these results, Strateole-2 balloons equipped with specialized sensors  
 72 were launched in the tropics in late 2021 with flight levels within the TTL and lower strato-  
 73 sphere. A new measurement platform named the Reel-down Atmospheric Temperature  
 74 Sensor (RATS), which senses temperature at the isopycnic balloon level and hundreds of  
 75 meters below the balloon level had its maiden flight November-December 2021. The goal  
 76 of these measurements is to characterize tropical waves in the short vertical wavelength  
 77 range that straddles the limits of ERA5 resolution. For this study we use RATS data  
 78 in conjunction with balloon level Thermodynamical SENSor (TSEN) observations (Hertzog  
 79 et al., 2004) to characterize tropical waves near 18 km in the lowermost tropical strato-  
 80 sphere. We use these unique measurements and ERA5 fields, to characterize tropical waves  
 81 above the Indian Ocean in the lowermost tropical stratosphere and study their repre-  
 82 sentation in ERA5.

## 83 2 Data and Instruments

### 84 2.1 Strateole-2 in situ TSEN observations

85 For Strateole-2, 25 super-pressure balloons were launched during two campaigns  
 86 from the Seychelles. The first campaign took place from November 2019 to February 2020  
 87 and the second campaign from October 2021 to January 2022. These balloons circum-  
 88 navigate the equator at 18 km or 20 km (Haase et al., 2018; Corcos et al., 2021). We fo-  
 89 cus on balloons C1-15-TTL4 (TTL4) and C1-16-TTL5 (TTL5) where both balloons are  
 90 equipped with the TSEN temperature sensor at floating level (Hertzog et al., 2004) and  
 91 the TTL5 balloon additionally carried the RATS instrument (see Fig. 1a). The TTL5  
 92 super-pressure flight duration was approximately 42 days and RATS was operational for  
 93 the first 16 days of the flight. Due to closely spaced launch times ( $< 2$  hr) and near-identical  
 94 float altitudes, the TTL4 and TTL5 balloons were floating in close proximity over the  
 95 course of 10 days (see Fig. 1a and c). This permits combination of the in-situ observa-  
 96 tions of these two balloons for the purpose of analyzing the horizontal wavelengths of  
 97 tropical waves.

98 In-situ balloon observations of ambient temperature, pressure and horizontal wind  
 99 vectors at the isopycnic floating levels of the Strateole-2 balloons were done with TSEN.  
 100 Wind speeds are calculated from the GPS position of the drifting balloon gondola. The  
 101 temperature sensor accuracy is 0.1 K at night and 0.25 K during the day after correction  
 102 for solar radiation (Hertzog et al., 2004). The precision of TSEN temperatures is on av-  
 103 erage about 4 mK for night-time measurements and about 20 mK for daytime, respec-  
 104 tively (Wilson et al., 2023). The absolute accuracy and precision of the pressure sensor  
 105 are  $\pm 2$  hPa and 0.01 hPa. Winds are derived from position with  $0.1 \text{ ms}^{-1}$  precision. The  
 106 temporal resolution of this data set is 30 s.

107

## 2.2 RATS

108

109

110

111

112

113

114

115

116

117

118

119

120

121

122

123

124

125

126

127

RATS is a platform designed to make simultaneous, continuous and fast-response measurements of temperature, pressure, and position at two altitudes from a drifting high-altitude balloon using the TSEN temperature and GPS (Fig. 1b). The temperature sensors were separated vertically by a reel-down cable, with one TSEN at the "Euros" control gondola flight level and the other at the end of the reel-down cable. The lower sensor was attached to a suspended sub-gondola, or end-of-fiber-unit (EFU). For the TTL5 flight, the separation length was about 200 m, but other lengths are possible on future flights. The flight level gondola contained the data and communications interface of RATS in addition to the mechanical reeling system used to deploy the EFU, which is identical to the reel system used by the FLOATS instrument (Goetz et al., 2023). The EFU design and implementation was also identical to FLOATS, with the TSEN probe located on a thin white PTFE wire about 1 m below the EFU sub-gondola. Other specifications can be found in (Goetz et al., 2023). Additionally, the same 600  $\mu\text{m}$  diameter liquid crystal polymer (LCP) coated fiber optic cable used for FLOATS was used to suspend the EFU. Its UV radiation exposure rating and breaking strain meet the International Civil Aviation Organization (ICAO) regulatory standards (i.e. Rules of the Air ICAO Appendix 4 Annex 2). For TTL5 the EFU was configured to transmit GPS position and TSEN pressure and temperature every 10 to 30 s via Long Range (LoRa) radio to the flight level gondola interface system. The Euros level TSEN and GPS was configured to a sampling period of 30 s and the EFU data was synced to the same clock.

128

## 2.3 ERA5 in Balloon Trajectory-Following Coordinates

129

130

131

132

133

ERA5 is an atmospheric reanalysis available at 6 hour intervals on 137 vertical levels up to 1hPa (Hersbach et al., 2020). The distance between the different vertical levels is about 400 m in the lower stratosphere and the horizontal resolution is 31 km. For this study the hourly ERA5 data was interpolated both in space and time to the balloon flight tracks of TTL4 and TTL5, respectively.

134

## 3 Methods

135

136

137

138

139

To determine the vertical or horizontal wavelengths we generally follow the approach of previous studies (Alexander et al., 2008; Wright et al., 2010; Ern et al., 2014; Alexander, 2015) who used adjacent satellite-borne temperature profiles to infer horizontal wavelengths. However for RATS analysis, we take into account covariance between two temperature time series rather than covariance between adjacent vertical profiles.

140

### 3.1 RATS vertical wavelength estimates

141

142

143

144

145

To calculate vertical wavelengths we use the temperatures measured with RATS ( $\sim 200$  m below balloon flight level) and TSEN (at balloon floating level) systems. We decompose the temperature observations into time  $t$  and frequency  $\omega$  spectrum applying the Stockwell transform (Stockwell et al., 1996). The covariance between the two spectra  $C_{TR}$  can be written as

146

$$C_{TR}(t, \omega) = \hat{T}_t \hat{T}_r^* \quad (1)$$

147

148

149

where the  $\hat{T}_t$  and  $\hat{T}_r^*$  are the complex temperature amplitude spectra observed by TSEN at balloon level and by RATS  $\sim 200$  m below the balloon, respectively. (See Fig.1b.) The star denotes the complex conjugate of  $\hat{T}_r$ . The phase shift is computed with

150

$$\Delta\phi_{TR} = \arctan\left(\frac{\text{Im}(C_{TR})}{\text{Re}(C_{TR})}\right) \quad (2)$$

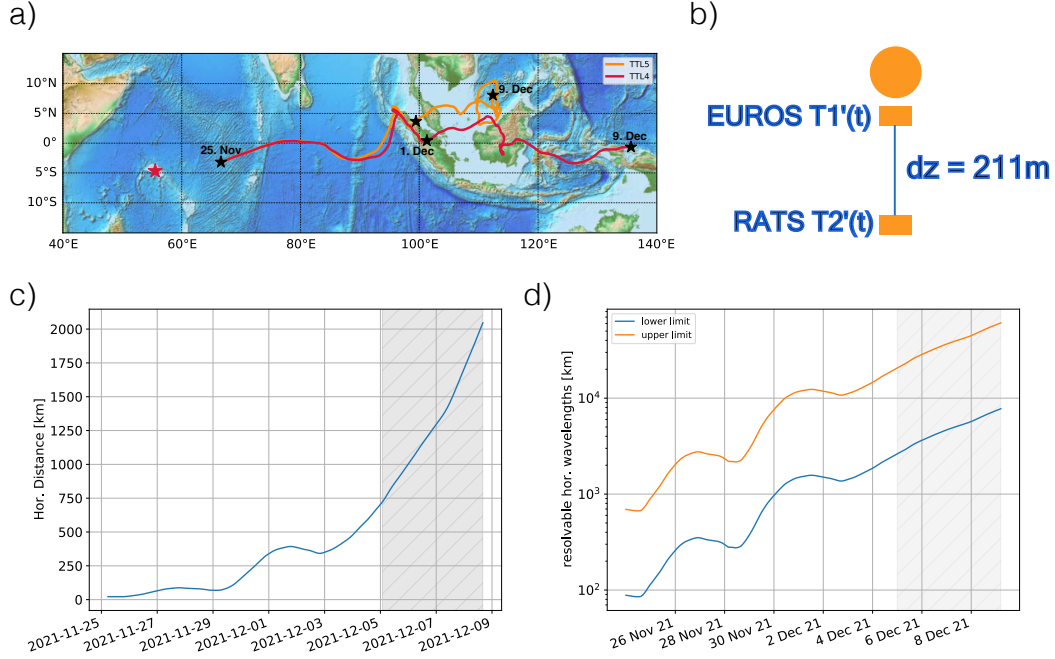


**Figure 1.** (a) Flight track of the TTL4 (red) and TTL5 (orange) balloons from 25th November to 9th December. The stars show the balloon positions on the 25th November, 1st December and 9th December, respectively. The red star highlights the Seychelles islands where the balloons were launched. (b) Schematic of TTL5 temperature measurements where RATS is on average 211m below the balloon. (c) Horizontal distance between the two balloons between 25th November and 9th December. (d) Theoretical upper and lower limits of horizontal wavelengths that can be resolved based on the horizontal distance of the balloons. Grey shading indicates the time period where the horizontal distance was too large and the data was excluded from the analysis.

151 From the vertical phase shift  $\Delta\phi_{TR}$  and the vertical distance  $\Delta_z = 211$  m we can then  
 152 estimate the vertical wavelength

$$153 \quad \lambda_z = \frac{\Delta\phi_{TR}}{\Delta_z}. \quad (3)$$

154 Due to the sensitivity of the instrument and to avoid aliasing effects we define wave pack-  
 155 ets with a covariance threshold  $> 0.5 K^2$  and only compute vertical wavelengths where  
 156 the observed phase difference  $|\Delta\phi_{TR}|$  is in the range  $0.2 - \pi$ .

157 As the vertical distance between the RATS and balloon observed temperatures is  
 158 a constant the resolvable vertical wavelengths range from  $\sim 420$  m to 6.6 km throughout  
 159 the observation period.

### 160 3.2 Dual-balloon horizontal wavelength estimates

161 As the balloons TTL4 and TTL5 were floating in close proximity over 10 days we  
 162 can also estimate the horizontal wavelength  $\lambda_x$  analogous to the vertical wavelength. In  
 163 this case the equation changes to

$$164 \quad \lambda_x = \frac{\Delta\phi_{45}}{\Delta_x(t)} \quad (4)$$

165 where  $\Delta\phi_{45}$  is the phase shift derived from the co-spectral analysis of TTL4 and TTL5  
 166 measured in-situ temperatures at the Euros gondola level and  $\Delta_x(t)$  is the horizontal dis-  
 167 tance between the two balloons which varies with time (see Fig.1c). As the horizontal

168 distance between the two balloons varies with time the resolvable horizontal wavelength  
 169 range changes accordingly (see Fig.1d). Note, we limit the application of this method  
 170 to times where  $\Delta_x$  is smaller than 750 km and where the change in time of  $\Delta_x$  is also  
 171 small. Also note that compared to their horizontal separation, the mean vertical distance  
 172 between the two balloons was negligibly small and is neglected in the analysis.

## 173 4 Results

### 174 4.1 Vertical and horizontal wavelength estimates from balloon obser- 175 vations

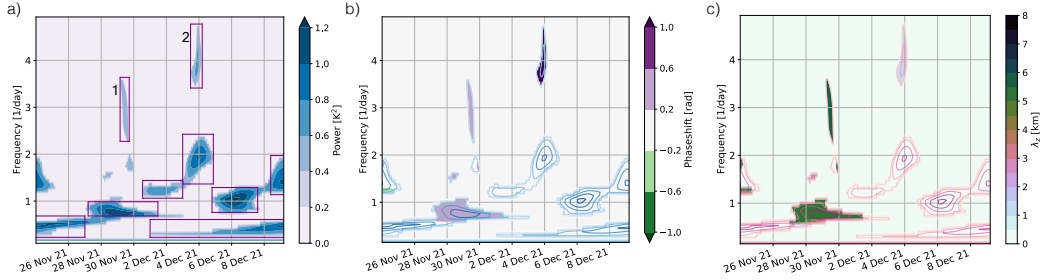


**Figure 2.** (a) Covariance of the temperatures measured by RATS and TSEN with a mask to only show significant amplitudes (power  $> 0.5K^2$ ). (b) Phase shift for significant wave packets with overlain covariance contours for reference. (c) Vertical wavelength for wave packets with detectable signals (where phase shift  $> 0.2$  radians). All spectra are shown as a function of time and wave frequency.

176 The covariance calculated from RATS and balloon flight-level observed tempera-  
 177 tures shows enhanced power for waves with periods between 12 hours and 2.5 days be-  
 178 tween 25th November 2021 and 8th December 2021 (Fig. 2a). Boxes on the figure iden-  
 179 tify potential candidate wave packets for analysis. The corresponding phase shifts, com-  
 180 puted as amplitude-weighted averages for each packet, reveal two high-frequency waves  
 181 and one low-frequency wave packet with detectable phase shifts in these measurements  
 182 (Fig. 2b). For these wave packets the vertical wavelengths range from 1.5 km to 5.5 km  
 183 (Fig. 2c). For wave packets with a vertical wavelength larger than 6.6 km the phase shift  
 184 becomes so small that it cannot be detected with the deployed instrument configuration.

185 Over the course of 10 days the balloons TTL4 and TTL5 floated in close proxim-  
 186 ity ( $\Delta x < 750$  km) allowing the analysis of horizontal wavelengths (see Fig. 3). Again the  
 187 covariance shows wave packet signals for periods between 5 hours and 2 days and phase  
 188 shifts are detectable ( $> 0.2$ ) especially for wave packets after 30 November 2021. The es-  
 189 timated horizontal wavelengths range between 500 km and 3000 km (see Fig. 3c). Note,  
 190 that the horizontal distance between the two balloons varies with time (see Fig. 1a and  
 191 c) which means that changes in the derived horizontal wavelengths over a wave packet  
 192 could be related to the change of horizontal distance between the balloons with time if  
 193 the wavelength shifts in or out of the observable range (see Eq.4 and Fig.1d).

### 194 4.2 Comparison to ERA5 reanalyses

195 As a next step we compare the observed covariances with ERA5 temperature cov-  
 196 ariances. For the comparison with the vertical RATS-TTL5 covariances we choose the  
 197 two ERA5 model levels that are closest to the balloon and RATS floating level. Please  
 198 note that the vertical grid spacing of ERA5 at this altitude region is about 350 m whereas

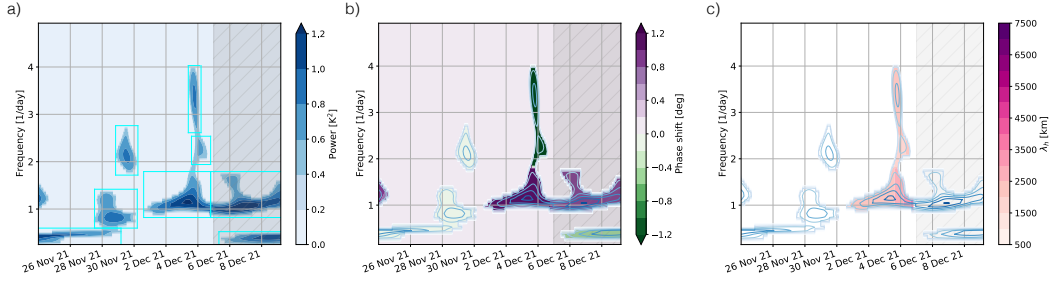


**Figure 3.** (a) Covariance of the temperatures measured by TTL4 and TTL5 TSEN with a mask to only show significant amplitudes (power  $> 0.5K^2$ ). (b) Phase shift between the temperatures for significant wave packets. (c) Resulting horizontal wavelength for significant wave packets and phase shift  $> 0.2$  radians. All spectra are shown as a function of time and wave frequency. Grey shaded areas highlight the time where the horizontal distance exceeds the threshold.

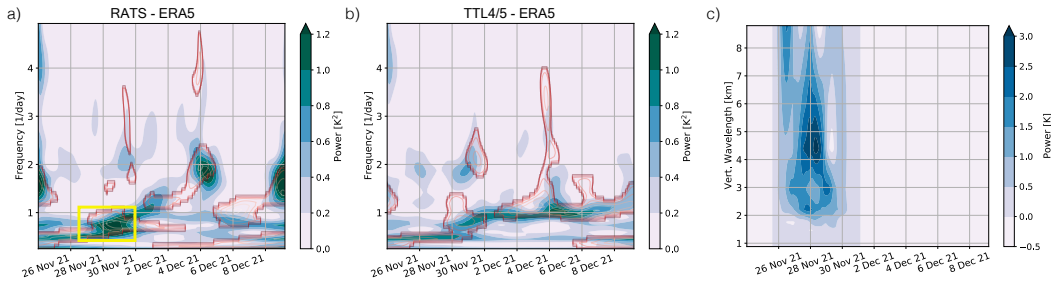


**Figure 4.** (a) Covariance of ERA5 temperatures between the two model levels that are closest to the balloon and RATS floating levels (blue and green contours). (b) Covariance of ERA5 temperatures interpolated to the TTL4 and TTL5 flight tracks. For both panels (a) and (b) the red contours identify where observed covariances  $> 0.5K^2$  as presented in Fig. 2a and 3a. (c) ERA5 vertical wavelength spectrum for the wave packet for which the best agreement between measurements and ERA5 was found (yellow box in panel (a)). The spectra in a) and b) are shown as a function of time and wave frequency.

199 RATS is only about 200 m below the balloon. For the comparison with the observed TTL4  
 200 and TTL5 covariances we use ERA5 data interpolated in space and time to the respec-  
 201 tive balloon flight tracks.

202 Fig. 4a shows that for frequencies lower than 2 cycles/day the ERA5 simulated co-  
 203 variances have similar structures and energies as the observed ones. This is especially  
 204 true for the wavepacket observed on 29th November 2021 with a frequency of  $\sim 0.6$  cycles/day  
 205 (see yellow box in Fig 4a). This similarity gives confidence in the wave-packet analysis  
 206 based on RATS observations, since the two figures Fig. 2a and Fig. 4a show correlations  
 207 obtained with independent datasets. However, most of the ERA5 wave packets seem to  
 208 evolve differently in time compared to observations and the observed high-frequency wave  
 209 packets (29th November and 3rd December) are not resolved at all in ERA5.

210 For the wave packed that is well reproduced in ERA5 (yellow box in Fig 4a) we cal-  
 211 culated the vertical wavelength for comparison with vertical wavelength estimates from  
 212 RATS. For this analysis we interpolated ERA5 data on an equal-spaced vertical grid and  
 213 then calculated the power spectrum of the vertical wavelength as a function of time (see



214 Fig. 4c). Most of the power is concentrated at a vertical wavelength of about 4.5 km which  
 215 is similar to the estimated 5 km vertical wavelength derived from RATS observations.

216 Comparing the ERA5 and observed covariances of TTL4 and TTL5 (Fig.4b) we  
 217 draw similar conclusions. Again, for low frequencies, less than 1/day, there is similar power  
 218 and temporal evolution, but the power for higher-frequency wave packets is underesti-  
 219 mated in ERA5 and temporal evolution does not much resemble the observations. As  
 220 ERA5 does not reproduce the observed packets that were well-resolved ( $\sim 3$  December  
 221 in Fig.4b), we do not attempt to compare the horizontal wavelengths between ERA5 and  
 222 observations.

## 223 5 Conclusions & Discussion

224 In this study we present first results of a newly developed instrument RATS (Reel-  
 225 down Atmospheric Temperature Sensor). RATS was developed during the second Strateole-  
 226 2 campaign in 2021 and this study provides a proof-of-concept analysis of first measure-  
 227 ments with this instrument. In its current design RATS was deployed about 200 m be-  
 228 low the balloon gondola thus enabling observations of tropical waves with vertical wave-  
 229 lengths between  $\sim 400$  m and 6 km. A previous study of long-duration balloon observa-  
 230 tions (Bramberger et al., 2022) found significant gravity waves with vertical wavelengths  
 231  $< 1$  km. In the present case study, we observed tropical waves with vertical wavelengths  
 232 between 1.5 km and 5 km. To extend the range of observable tropical waves future plans  
 233 include the development of several RATS instruments allowing different vertical distances.  
 234 These different RATS instruments can be deployed on several balloons in the next Strateole-  
 235 2 campaign planned for late 2025.

236 The comparison to ERA5 reanalyses shows that the power distribution in the co-  
 237 variances at frequencies  $\leq 1$  cycle/day is similar to the observations, both for the RATS  
 238 and the TTL4/TTL5 comparisons. However, the power is underestimated for high-frequency  
 239 waves with frequencies  $\geq 2$  cycles/day, and some prominent observed higher frequency  
 240 waves are absent in ERA5. Given the limited 10-day time series in this study, it is pos-  
 241 sible some higher frequency wave events may appear in ERA5 but with different tim-  
 242 ing than in the observations. The differences might be related to modeling limitations  
 243 due to limited vertical resolution or differences in ERA5 representation of convection,  
 244 which is the likely source of these tropical gravity waves (Corcos et al., 2021). Never-  
 245 theless, one low-frequency wave packet compared very well between ERA5 and RATS  
 246 observations and we could therefore compare the respective vertical wavelengths. The  
 247 found wavelengths agree well between ERA5 and RATS which adds confidence to the  
 248 analysis technique applied to the RATS data.

249 Momentum fluxes calculated with a previously published method (Corcos et al.,  
 250 2021) for the two high-frequency wave packets 1 and 2 in Fig.2a are modest with about  
 251  $\sim 1$  mPa and  $\sim 5$  mPa, respectively. The found momentum fluxes are in concurrence with  
 252 Corcos et al. (2021) where 1-5 mPa were the most commonly observed values and the  
 253 global average momentum flux was  $\sim 5$  mPa. In their study they found that collectively  
 254 the high-frequency waves ( $> 1$  cycle/day) contribute at least 25%, and possibly more than  
 255 50%, to the total force required to drive the QBO.

256 In general, there is good correspondence in the temperature covariance time series  
 257 comparing the balloons to ERA5 for inertia-gravity waves with periods in the 1-2 day  
 258 range. Similar signals were analyzed in ERA5 in detail over decades (Pahlavan, Fu, et  
 259 al., 2021), and finding their contribution to forcing the QBO. Our comparison to these  
 260 balloon data suggests these low-frequency gravity waves may be quite realistic in ERA5,  
 261 both in their locations, timing, and amplitude (Fig.4). However, although this is only  
 262 a limited case study comparison, the ERA5 reanalysis appears to be deficient in grav-  
 263 ity waves at higher frequencies. Additionally, ERA5 vertical resolution limitations were

264 implicated in missing waves seen in a previous balloon study (Bramberger et al., 2022)  
 265 that should otherwise have been resolvable. Future comparisons between Strateole-2 bal-  
 266 loon observations and reanalyses should further illuminate the strengths and limitations  
 267 of the reanalysis datasets for representing tropical gravity waves.

## 268 Acknowledgments

269 The TSEN and RATS data were collected as part of Strateole-2, which is sponsored by  
 270 CNES, CNRS/INSU and NSF. Joan Alexander and Martina Bramberger were supported  
 271 by NSF grants 1642246 and 1642644. Development of FLOATS/RATS was supported  
 272 by NSF award 1419932 and deployment was supported by NSF award 1642277. The au-  
 273 thors would like to acknowledge Agustin Caro, the LATMOS gondola team, and Karim  
 274 Ramage for their expertise and patience in the field. We give special thanks to Stephanie  
 275 Venel and the CNES ballooning team for their exceptional balloon launches, profession-  
 276 alism, and for making these difficult measurements possible.

## 277 References

- 278 Alexander, M. J. (2015). Global and seasonal variations in three-dimensional gravity  
 279 wave momentum flux from satellite limb-sounding temperatures. *Geophys. Res.*  
 280 *Lett.*, *42*(16), 6860-6867. doi: 10.1002/2015GL065234
- 281 Alexander, M. J., Gille, J., Cavanaugh, C., Coffey, M., Craig, C., Eden, T., ...  
 282 Dean, V. (2008). Global estimates of gravity wave momentum flux from high  
 283 resolution dynamics limb sounder observations. *J. Geophys. Res. Atmos.*,  
 284 *113*(D15). doi: <https://doi.org/10.1029/2007JD008807>
- 285 Bramberger, M., Alexander, M. J., Davis, S., Podglajen, A., Hertzog, A., Kalnajs,  
 286 L., ... Khaykin, S. (2022). First super-pressure balloon-borne fine-  
 287 vertical-scale profiles in the upper ttl: Impacts of atmospheric waves on cir-  
 288 rus clouds and the qbo. *Geophys. Res. Lett.*, *49*(5), e2021GL097596. doi:  
 289 <https://doi.org/10.1029/2021GL097596>
- 290 Corcos, M., Hertzog, A., Plougonven, R., & Podglajen, A. (2021). Observation of  
 291 Gravity Waves at the Tropical Tropopause Using Superpressure Balloons. *J.*  
 292 *Geophys. Res. Atmos.*, *126*(15), e2021JD035165. doi: [https://doi.org/10.1029/](https://doi.org/10.1029/2021JD035165)  
 293 [2021JD035165](https://doi.org/10.1029/2021JD035165)
- 294 Davis, S. M., Hegglin, M. I., Fujiwara, M., Dragani, R., Harada, Y., Kobayashi, C.,  
 295 ... Wright, J. S. (2017). Assessment of upper tropospheric and stratospheric  
 296 water vapor and ozone in reanalyses as part of s-rip. *Atmospheric Chemistry*  
 297 *and Physics*, *17*(20), 12743–12778. doi: 10.5194/acp-17-12743-2017
- 298 Ern, M., Ploeger, F., Preusse, P., Gille, J. C., Gray, L. J., Kalisch, S., ... Riese, M.  
 299 (2014). Interaction of gravity waves with the QBO: A satellite perspective. *J.*  
 300 *Geophys. Res. Atmos.*, *119*(5), 2329-2355. doi: 10.1002/2013JD020731
- 301 Garfinkel, C. I., Gerber, E. P., Shamir, O., Rao, J., Jucker, M., White, I., & Paldor,  
 302 N. (2022). A QBO Cookbook: Sensitivity of the Quasi-Biennial Oscilla-  
 303 tion to Resolution, Resolved Waves, and Parameterized Gravity Waves. *J.*  
 304 *Adv. Model. Earth Syst.*, *14*(3), e2021MS002568. Retrieved from [https://](https://agupubs.onlinelibrary.wiley.com/doi/abs/10.1029/2021MS002568)  
 305 [agupubs.onlinelibrary.wiley.com/doi/abs/10.1029/2021MS002568](https://doi.org/10.1029/2021MS002568) doi:  
 306 <https://doi.org/10.1029/2021MS002568>
- 307 Goetz, J. D., Kalnajs, L. E., Deshler, T., Davis, S. M., Bramberger, M., & Alexan-  
 308 der, M. J. (2023). A fiber-optic distributed temperature sensor for continuous  
 309 in situ profiling up to 2 km beneath constant-altitude scientific balloons. *At-*  
 310 *mos. Meas. Tech.*, *16*(3), 791–807. doi: 10.5194/amt-16-791-2023
- 311 Haase, J., Alexander, M., Hertzog, A., Kalnajs, L., Deshler, T., Davis, S., ... Venel,  
 312 S. (2018). Around the world in 84 days. *EOS*, *99*. doi: [https://doi.org/](https://doi.org/10.1029/2018EO091907)  
 313 [10.1029/2018EO091907](https://doi.org/10.1029/2018EO091907)
- 314 Hersbach, H., Bell, B., Berrisford, P., Hirahara, S., Horányi, A., Muñoz Sabater,

- 315 J., ... Thópaút, J.-N. (2020). The ERA5 global reanalysis. *Quart. J. Roy.*  
 316 *Meteor. Soc.*, 146(730), 1999-2049. doi: <https://doi.org/10.1002/qj.3803>
- 317 Hertzog, A., Basdevant, C., Vial, F., & Mechoso, C. R. (2004). The accuracy  
 318 of stratospheric analyses in the northern hemisphere inferred from long-  
 319 duration balloon flights. *Q.J.R. Meteorol. Soc.*, 130(597), 607-626. doi:  
 320 <https://doi.org/10.1256/qj.03.76>
- 321 Holt, L. A., Lott, F., Garcia, R. R., Kiladis, G. N., Cheng, Y.-M., Anstey, J. A.,  
 322 ... Yukimoto, S. (2020). An evaluation of tropical waves and wave forc-  
 323 ing of the QBO in the QBOi models. *Q J R Meteorol Soc.*, n/a(n/a). doi:  
 324 <https://doi.org/10.1002/qj.3827>
- 325 Jensen, E. J., Pfister, L., Jordan, D. E., Bui, T. V., Ueyama, R., Singh, H. B., ...  
 326 Pfeilsticker, K. (2017). The NASA Airborne Tropical TRopopause EXper-  
 327 iment: High-Altitude Aircraft Measurements in the Tropical Western Pacific.  
 328 *Bull. Am. Meteorol. Soc.*, 96, 129-143. doi: [doi:10.1175/BAMS-D-14-00263.1](https://doi.org/10.1175/BAMS-D-14-00263.1)
- 329 Kalnajs, L. E., Davis, S. M., Goetz, J. D., Deshler, T., Khaykin, S., St. Clair, A.,  
 330 ... Lykov, A. (2021). A reel-down instrument system for profile measure-  
 331 ments of water vapor, temperature, clouds, and aerosol beneath constant-  
 332 altitude scientific balloons. *Atmos. Meas. Tech.*, 14(4), 2635-2648. doi:  
 333 [10.5194/amt-14-2635-2021](https://doi.org/10.5194/amt-14-2635-2021)
- 334 Kim, J.-E., & Alexander, M. J. (2015). Direct impacts of waves on tropical cold  
 335 point tropopause temperature. *Geophys. Res. Lett.*, 42(5), 1584-1592. doi: [10.1002/2014GL062737](https://doi.org/10.1002/2014GL062737)
- 336  
 337 Kim, J.-E., Alexander, M. J., Bui, T. P., Dean-Day, J. M., Lawson, R. P., Woods,  
 338 S., ... Jensen, E. J. (2016). Ubiquitous influence of waves on tropical  
 339 high cirrus clouds. *Geophysical Research Letters*, 43(11), 5895-5901. doi:  
 340 <https://doi.org/10.1002/2016GL069293>
- 341 Kim, Y.-H., & Chun, H.-Y. (2015). Momentum forcing of the quasi-biennial os-  
 342 cillation by equatorial waves in recent reanalyses. *Atmos. Chem. and Phys.*,  
 343 15(12), 6577-6587. doi: [10.5194/acp-15-6577-2015](https://doi.org/10.5194/acp-15-6577-2015)
- 344 Pahlavan, H. A., Fu, Q., Wallace, J. M., & Kiladis, G. N. (2021). Revisiting the  
 345 Quasi-Biennial Oscillation as Seen in ERA5. Part I: Description and Momen-  
 346 tum Budget. *J. Atmos. Sci.*, 78(3), 673 - 691. doi: [10.1175/JAS-D-20-0248.1](https://doi.org/10.1175/JAS-D-20-0248.1)
- 347 Pahlavan, H. A., Wallace, J. M., Fu, Q., & Kiladis, G. N. (2021). Revisiting the  
 348 quasi-biennial oscillation as seen in era5. part ii: Evaluation of waves and  
 349 wave forcing. *J. Atmos. Sci.*, 78(3), 693 - 707. doi: <https://doi.org/10.1175/JAS-D-20-0249.1>
- 350  
 351 Richter, J. H., Anstey, J. A., Butchart, N., Kawatani, Y., Meehl, G. A., Osprey,  
 352 S., & Simpson, I. R. (2020). Progress in simulating the quasi-biennial  
 353 oscillation in cmip models. *Journal Geophysical Research: Atmospheres*,  
 354 125(e2019JD032362). doi: [10.1029/2019JD032362](https://doi.org/10.1029/2019JD032362)
- 355 Richter, J. H., Butchart, N., Kawatani, Y., Bushell, A. C., Holt, L., Serva, F., ...  
 356 Yukimoto, S. (2020). Response of the Quasi-Biennial Oscillation to a warm-  
 357 ing climate in global climate models. *Quart. J. Roy. Meteor. Soc.*, 1-29. doi:  
 358 [10.1002/qj.3749](https://doi.org/10.1002/qj.3749)
- 359 Scaife, A. A., Baldwin, M. P., Butler, A. H., Charlton-Perez, A. J., Domeisen,  
 360 D. I. V., Garfinkel, C. I., ... Thompson, D. W. J. (2022). Long-range pre-  
 361 diction and the stratosphere. *Atmospheric Chemistry and Physics*, 22(4),  
 362 2601-2623. doi: [10.5194/acp-22-2601-2022](https://doi.org/10.5194/acp-22-2601-2022)
- 363 Solomon, S., Rosenlof, K., Portmann, R., Daniel, J., Davis, S., Sanford, T., &  
 364 Plattner, G.-K. (2010, 03). Contributions of Stratospheric Water Vapor to  
 365 Decadal Changes in the Rate of Global Warming. *Science*, 327, 1219-23. doi:  
 366 [10.1126/science.1182488](https://doi.org/10.1126/science.1182488)
- 367 Stockwell, R. G., Mansinha, L., & Lowe, R. P. (1996). Localization of the complex  
 368 spectrum: the S transform. *IEEE Transactions on Signal Processing*, 44(4),  
 369 998-1001. doi: [10.1109/78.492555](https://doi.org/10.1109/78.492555)

- 370 Ueyama, R., Schoeberl, M., Jensen, E., Pfister, L., Park, M., & Ryo, J.-M. (2023).  
 371 Convective impact on the global lower stratospheric water vapor budget. *Jour-*  
 372 *nal of Geophysical Research: Atmospheres*, *128*(6), e2022JD037135. doi:  
 373 <https://doi.org/10.1029/2022JD037135>
- 374 Vincent, R. A., & Alexander, M. J. (2020). Balloon-Borne Observations of Short  
 375 Vertical Wavelength Gravity Waves and Interaction With QBO Winds. *J.*  
 376 *Geophys. Res. Atmos.*, *125*(15), e2020JD032779. doi: 10.1029/2020JD032779
- 377 Wilson, R., Pitois, C., Podglajen, A., Hertzog, A., Corcos, M., & Plougonven, R.  
 378 (2023). Detection of turbulence occurrences from temperature, pressure, and  
 379 position measurements under superpressure balloons. *Atmos. Meas. Tech.*,  
 380 *16*(2), 311–330. doi: 10.5194/amt-16-311-2023
- 381 Wright, C. J., Osprey, S. M., Barnett, J. J., Gray, L. J., & Gille, J. C. (2010).  
 382 High resolution dynamics limb sounder measurements of gravity wave activ-  
 383 ity in the 2006 arctic stratosphere. *J. Geophys. Res. Atmos.*, *115*(D2). doi:  
 384 <https://doi.org/10.1029/2009JD011858>